Supplemental Figures

Figure S1. *Mir155*-deficient and WT mixed bone marrow chimeras are Th1 competent but have an intrinsic defect in Treg homeostasis.

Figure S2. Transcriptional control of *Mir155* and characterization of Th17 cultures with or without exogenous IL-1β.

Figure S3. *Mir155*-deficient Th17 cells have reduced expression of cytokines and increased c-Maf expression.

Figure S4. *Jarid2* is a conserved target of miR-155.

Figure S5. Target genes of Jarid2 and PRC2 in *Mir155*-deficient Th17 cells and analysis of *Atf3*-deficient Th17 cells.

Figure S6. *Jarid2* conditional targeting in $CD4^+$ T cells.

Figure S7. Profiling PRC2 and c-Maf binding at *Il22* and *Il10* locus in $Mir155^{-/-}$, double-deficient $Mir155^{-/-}$; $Jarid2^{-/-}$, and WT Th17 cell cultures, and updated Th17 network.

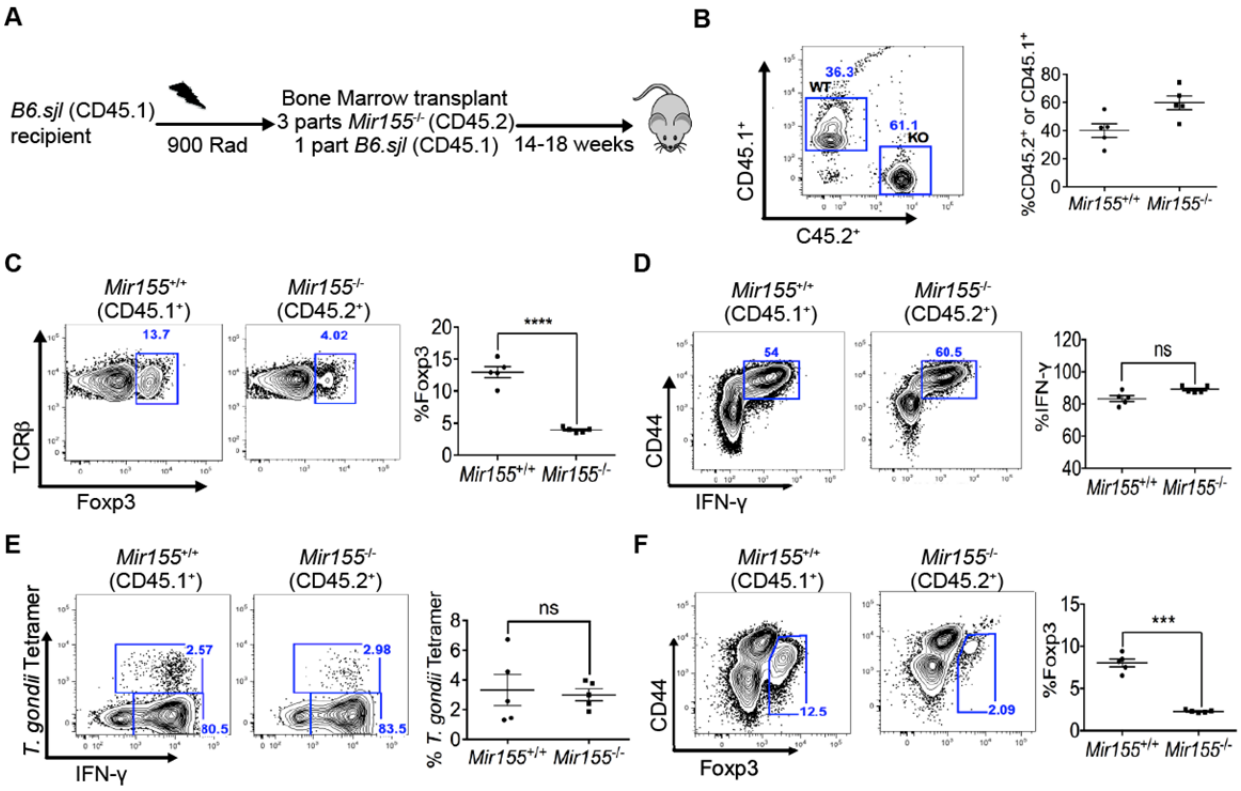

Figure S1, related to Figure 1. *Mir155*-deficient and WT mixed bone marrow (BM) chimeras are Th1 competent but have an intrinsic defect in Treg homeostasis. (A) Schematic of mixed BM chimera experiment. (B) FACS analysis of *Mir155*$^{-/-}$ (CD45.2^{+}) and *Mir155*$^{+/+}$ (CD45.1^{+}) cells from the mesenteric lymph node (MLN) of mixed BM chimera and the corresponding percentages of total lymphocytes that are either CD45.2^{+} or CD45.1^{+} after reconstitution. (C) FACS analysis of CD4^{+} *Mir155*$^{-/-}$ and *Mir155*$^{+/+}$ cells to enumerate TCRβ^{+} Foxp3^{+} cells in MLN of mixed BM chimeras and percent of CD4^{+}TCRβ^{+}Foxp3^{+} in *Mir155*$^{-/-}$ and *Mir155*$^{+/+}$ populations. (D) FACS analysis of CD4^{+}TCRβ^{+} *Mir155*$^{-/-}$ and *Mir155*$^{+/+}$ cells from MLN of infected mixed BM chimeras to enumerate IFN-γ producing cells, 8 days after initial *T. gondii* infection and corresponding percentages among *Mir155*$^{-/-}$ and *Mir155*$^{+/+}$ infected mixed BM chimeras. (E) FACS analysis of *Mir155*$^{-/-}$ and *Mir155*$^{+/+}$ CD4^{+}TCRβ^{+}CD44^{+} cells to enumerate IFN-γ expressing cells that can be stained with a *T. gondii* specific AS15 I-A^{b}

tetramer in MLN of infected mixed BM chimeras and percentages of AS15 I-A^b tetramer positive $CD4^+TCR\beta^+CD44^+IFN\text{-}\gamma^+$ cells among *Mir155*$^{-/-}$ and *Mir155*$^{+/+}$ population in the MLN of infected mixed BM chimeras. (F) FACS analysis of siLP $CD4^+TCR\beta^+CD44^+$ *Mir155*$^{-/-}$ and *Mir155*$^{+/+}$ cells expressing Foxp3 in *Toxoplasma gondii*-infected mixed BM chimeras and percentages of Foxp3 expressing cells among *Mir155*$^{-/-}$ and *Mir155*$^{+/+}$ $CD4^+TCR\beta^+CD44^+$ cells Results are representative of two independent cohorts that included four and five chimeras. Statistical significance was determined using Student's t test (**** $p<0.0001$).

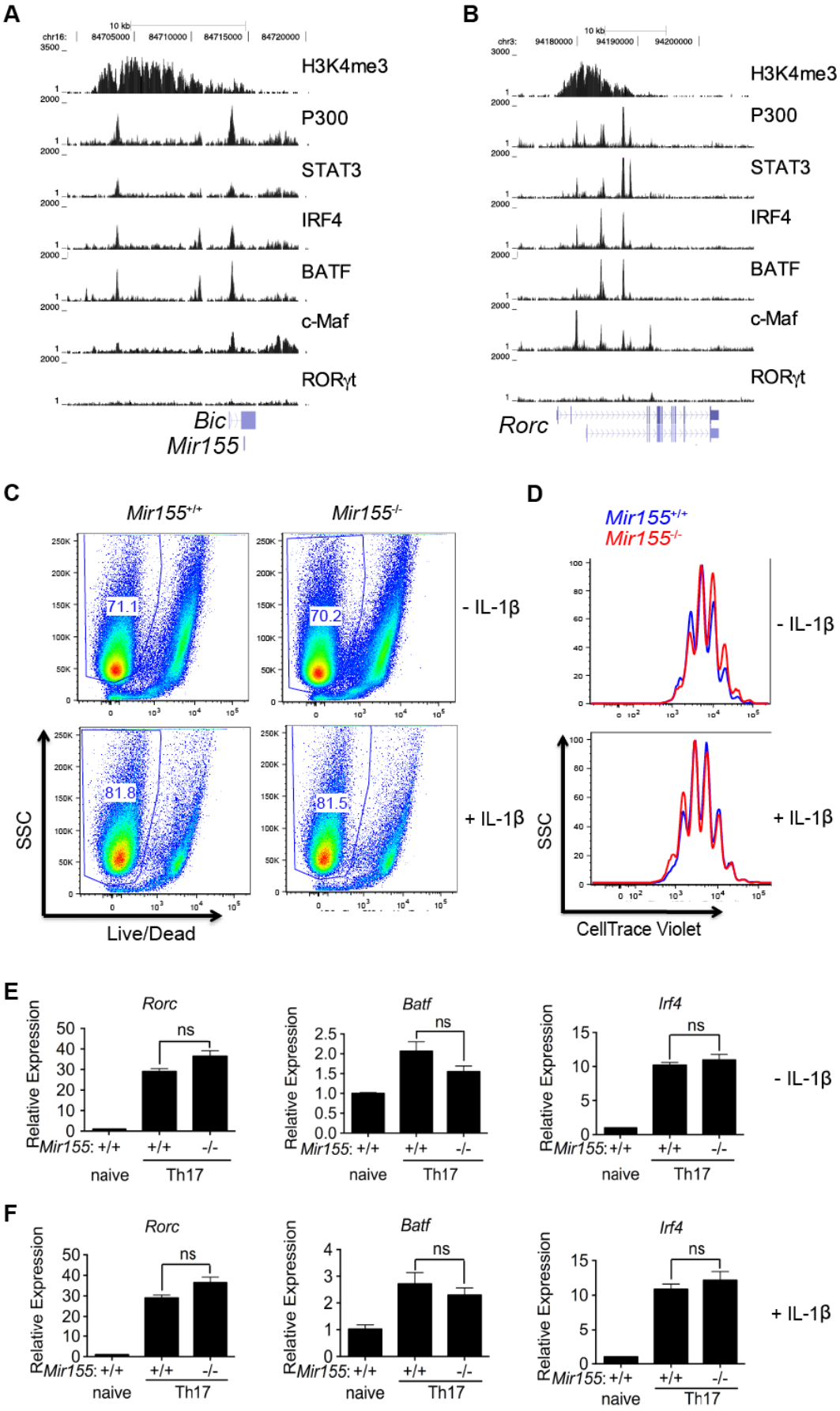
A
B
H3K4me3
P300
STAT3
IRF4
BATF
c-Maf
RORγt
Bic
Mir155
Rorc
C
Mir155+/+
Mir155-/-
71.1
70.2
81.8
81.5
- IL-1β
+ IL-1β
SSC
Live/Dead
D
CellTrace Violet
E
F
Relative Expression
Rorc
Batf
Irf4
ns
Mir155: +/+ +/+ -/-
naive
Th17

Figure S2, related to Figure 2. Transcriptional control of *Mir155* and characterization of Th17 cultures with or without exogenous IL-1β (A,B) Genome browser screen-shot of the mouse *Bic/Mir155* (A) and *Rorc* (B) locus depicting H3K4me3, P300, STAT3, IRF4, BATF, c-Maf and RORγt ChIP-seq of WT Th17 cultures. Primary data were downloaded from GSE40918 (Ciofani et al., 2012). (C) Representative FACS plots showing side scatter and Live/Dead stain of Th17 cell cultures polarized with or without exogenous IL-1β in *Mir155*$^{-/-}$ and *Mir155*$^{+/+}$ cell cultures. (D) Proliferation analyses of *Mir155*$^{-/-}$ and *Mir155*$^{+/+}$ cell cultures with or without exogenous IL-1β using CellTrace Violet dye. (E,F) RT-qPCR of *Rorc*, *Batf* and *Irf4* transcripts (E) without exogenous IL-1β or (F) with IL-1β. Relative expression was determined by normalizing to *Gapdh* mRNA and then to naïve CD4^{+} T cell expression. Statistical significance was determined using Student's t test (ns denotes not significant).

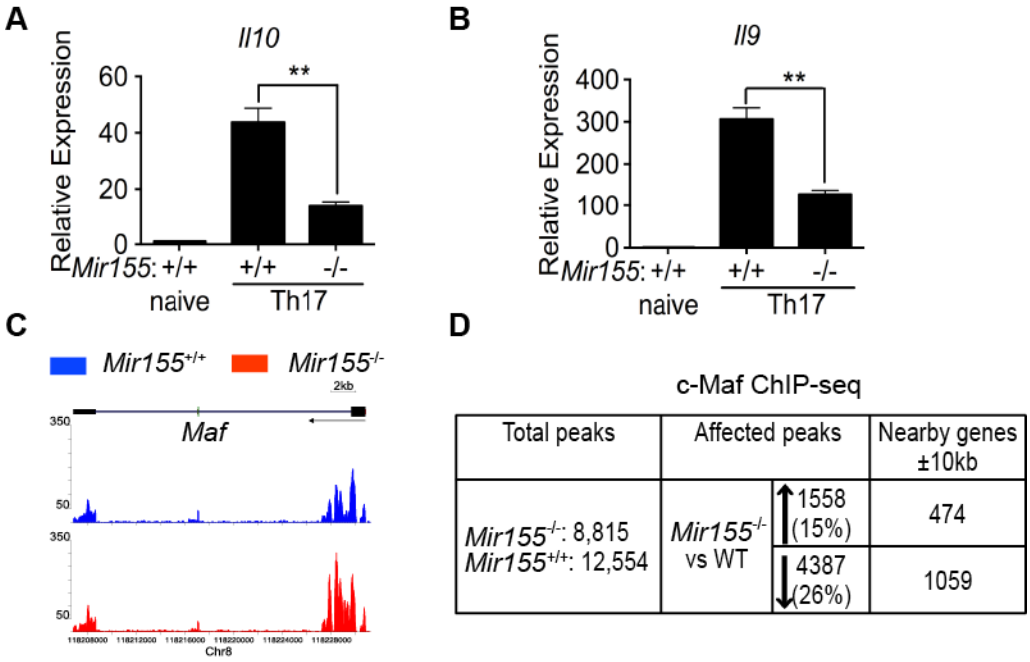

Total peaks	Affected peaks		Nearby genes ±10kb
Mir155$^{-/-}$: 8,815 *Mir155*$^{+/+}$: 12,554	*Mir155*$^{-/-}$ vs WT	↑ 1558 (15%)	474
		↓ 4387 (26%)	1059

Figure S3, related to Figure 3. *Mir155*-deficient Th17 cells have reduced expression of cytokines and increased c-Maf expression. RT-qPCR of *Il10* (A) and *Il9* (B) in *Mir155*$^{-/-}$ and

Mir155$^{+/+}$ Th17 cells differentiated with IL-1β. Relative expression was determined by normalizing to *Gapdh* mRNA and then to naïve CD4^{+} T cell expression. Statistical significance was determined using Student's t test (** $p<0.01$). (C) Genome browser screen shot of *Maf* (gene encoding c-Maf) expression in *Mir155*$^{-/-}$ and *Mir155*$^{+/+}$ Th17 determined by RNA-seq. (D) Table summarizes c-Maf ChIP-seq in *Mir155*$^{-/-}$ and *Mir155*$^{+/+}$ Th17 cell cultures. First column is total number of c-Maf peaks identified using MACS. Second column indicates the number of peaks affected (either↑or↓) in *Mir155*$^{-/-}$ with *Mir155*$^{+/+}$ as a control using MACS2.0. Third column indicates the number of RefSeq genes within 10 kb of the peaks in question.

A

Gene	FC
Bach1	2.3
H3f3a	1.5
Ikbke	1.4
Jarid2	1.5
Jhdm1d	1.8
Kpna1	1.6
Ptpn2	1.4
Rps6ka5	2.0
Sdcbp	1.8
Sla	1.4
Sp3	1.4
Tfdp2	1.5
Tle4	1.8
Trim2	2.1
Wee1	1.9

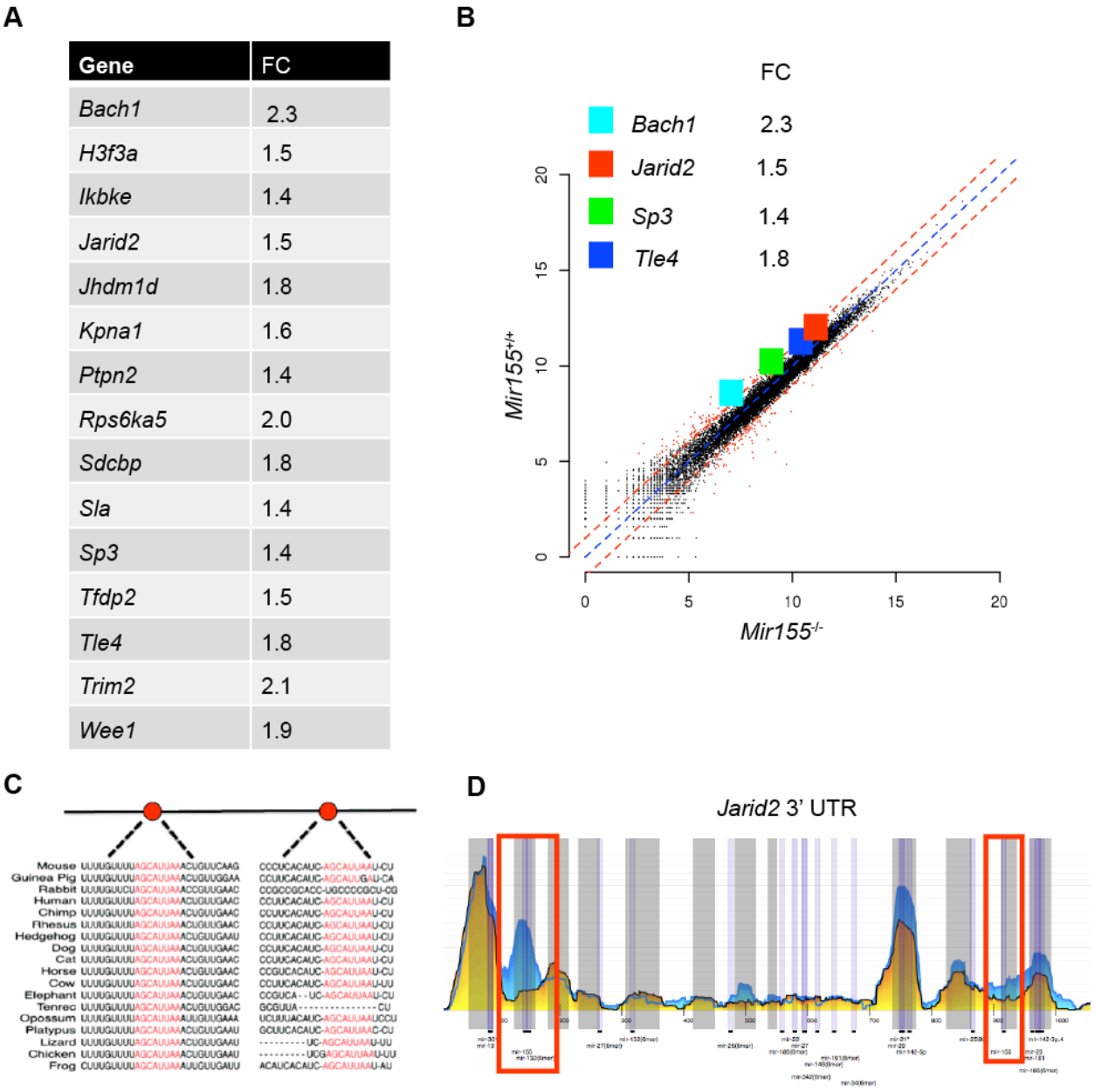

Figure S4, related to Figure 4. *Jarid2* is a conserved target of miR-155. (A) List of genes found in the intersection of Sylamer, TargetScan and Pictar analyses with their respective fold change in *Mir155*$^{-/-}$ compared to *Mir155*$^{+/+}$. Genes in bold type represent known transcriptional repressors. (B) Scatter-plot of gene expression from *Mir155*$^{-/-}$ and *Mir155*$^{+/+}$ Th17 RNA-seq highlighting the transcriptional repressors from (A). (C) A schematic of 3' UTR of *Jarid2* depicts the two conserved miR-155 binding sites and their sequence alignment across 18 species (data

obtained from TargetScan (Lewis et al., 2003). The putative miR-155 binding sequences are highlighted in red. (D) The 3' UTR of *Jarid2* in *Mir155*$^{-/-}$ (yellow) and *Mir155*$^{+/+}$ (Blue) Th0 cells from the high-throughput sequencing of RNA isolated by Ago2 crosslinking and immunoprecipitation (HITS-CLIP; http://cbio.mskcc.org/~aakhan/clipseq/) (Loeb et al., 2012). The red boxes highlight the two miR-155 binding sites from (A).

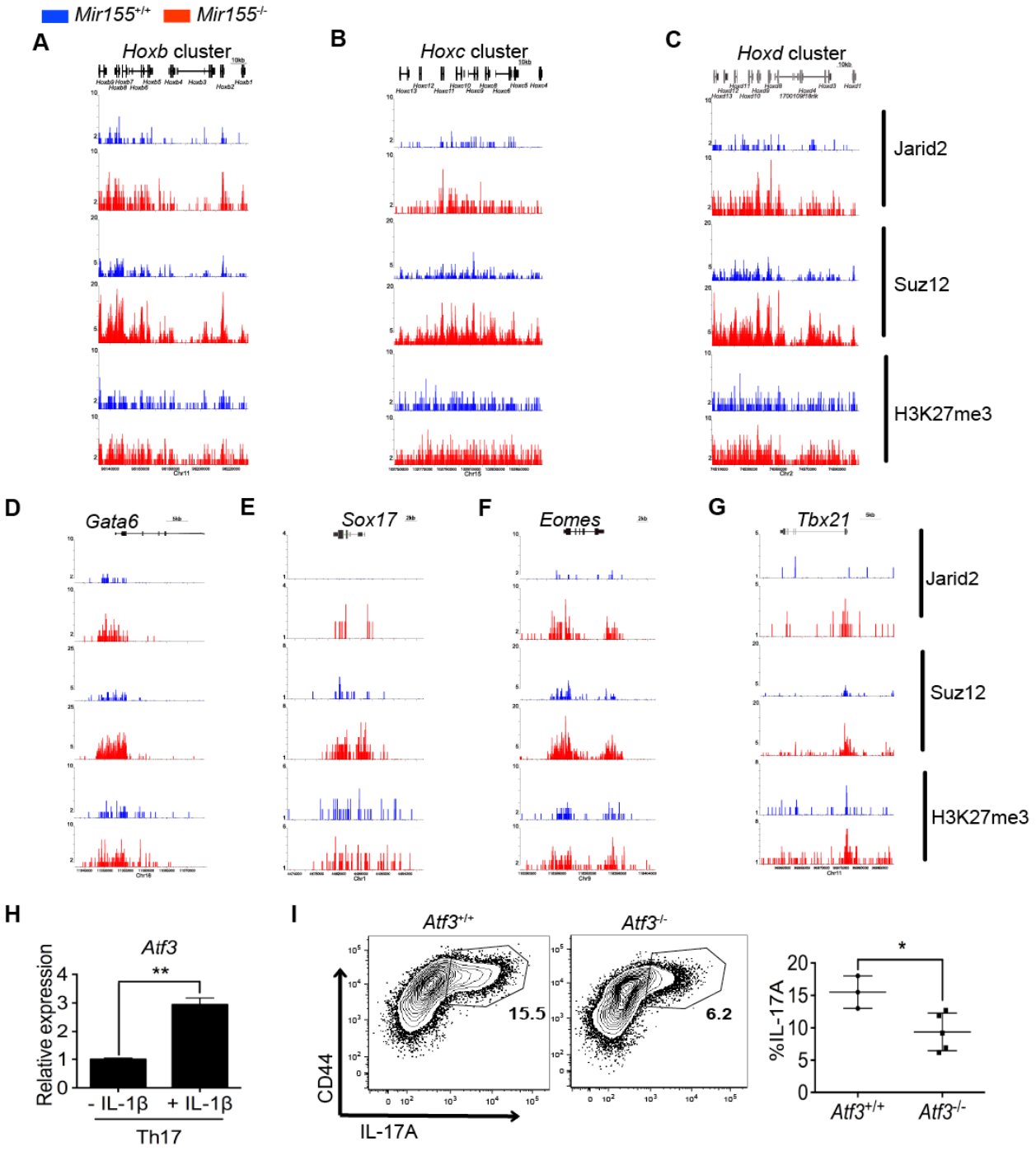

Figure S5, related to Figure 5. Target genes of Jarid2 and PRC2 in *Mir155*-deficient Th17 cells and analysis of *Atf3*-deficient Th17 cells. Genome browser screenshots depict Jarid2, Suz12, and H3K27me3 enrichment in the *HoxB* cluster (A), *HoxC* cluster (B), *HoxD* cluster (C), *Gata6* (D), *Sox17* (E), *Eomes* (F) and *Tbx21* (I) loci as a result of ChIP-seq experiments in

Mir155$^{-/-}$ (red) and *Mir155*$^{+/+}$ (blue) Th17 cells. (H) Relative expression of *Atf3* mRNA by RT-qPCR from 4-day WT Th17 cell cultures differentiated with or without exogenous IL-1β. (I) FACS analysis depicting CD44 and IL-17A expression in CD4^{+} T cells from *Atf3*$^{-/-}$ and WT Th17 cell cultures and corresponding percent of IL-17A. Statistical significance was determined using Student's t test ($**$ $p<0.01$ and $*$ $p<0.05$).

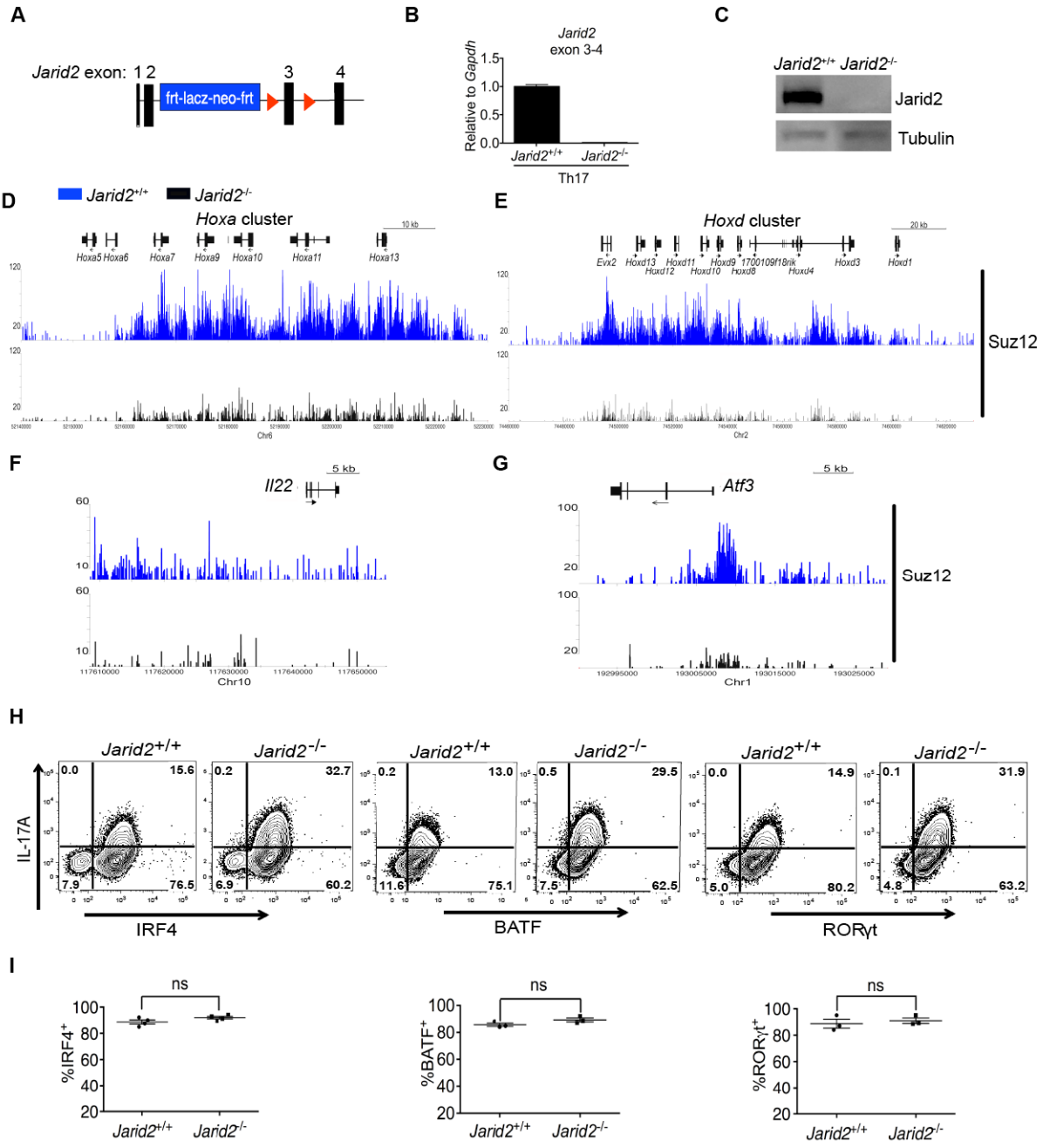

Figure S6, related to Figure 6. *Jarid2* conditional targeting in CD4$^+$ T cells. (A) Schematic of *Jarid2* conditional targeting. In this conditional allele, exon 3 is flanked by loxP sites in a strategy that is essentially identical to a previously published allele of *Jarid2* (Mysliwiec et al., 2006; Shen et al., 2009). (B) RT-qPCR across targeted exon 3 from *Jarid2*$^{-/-}$ (*Jarid2*$^{fl/fl}$; CD4-cre) and littermate controls. Relative expression was found by normalizing to *Gapdh* mRNA. (C)

Jarid2 western blot of *Jarid2*$^{-/-}$ and *Jarid2*$^{+/+}$ Th17 cell cultures. (D-G) Genome browser screenshots of the *HoxA* cluster (D), *HoxD* cluster (E), *Il22* (F), and *Atf3* (G) from the ChIP-exo of Suz12 in *Jarid2*$^{-/-}$ and *Jarid2*$^{+/+}$ Th17 cell cultures. (H) Representative FACS plots of RORγt, BATF, or IRF4 versus IL-17A intracellular expression. (I) Percentages of cells expressing RORγt, BATF, or IRF4 in *Jarid2*$^{-/-}$ and *Jarid2*$^{+/+}$ Th17 cell cultures. Results are representative of three independent experiments. Statistical significance was determined using Student's t test (ns denotes not significant).

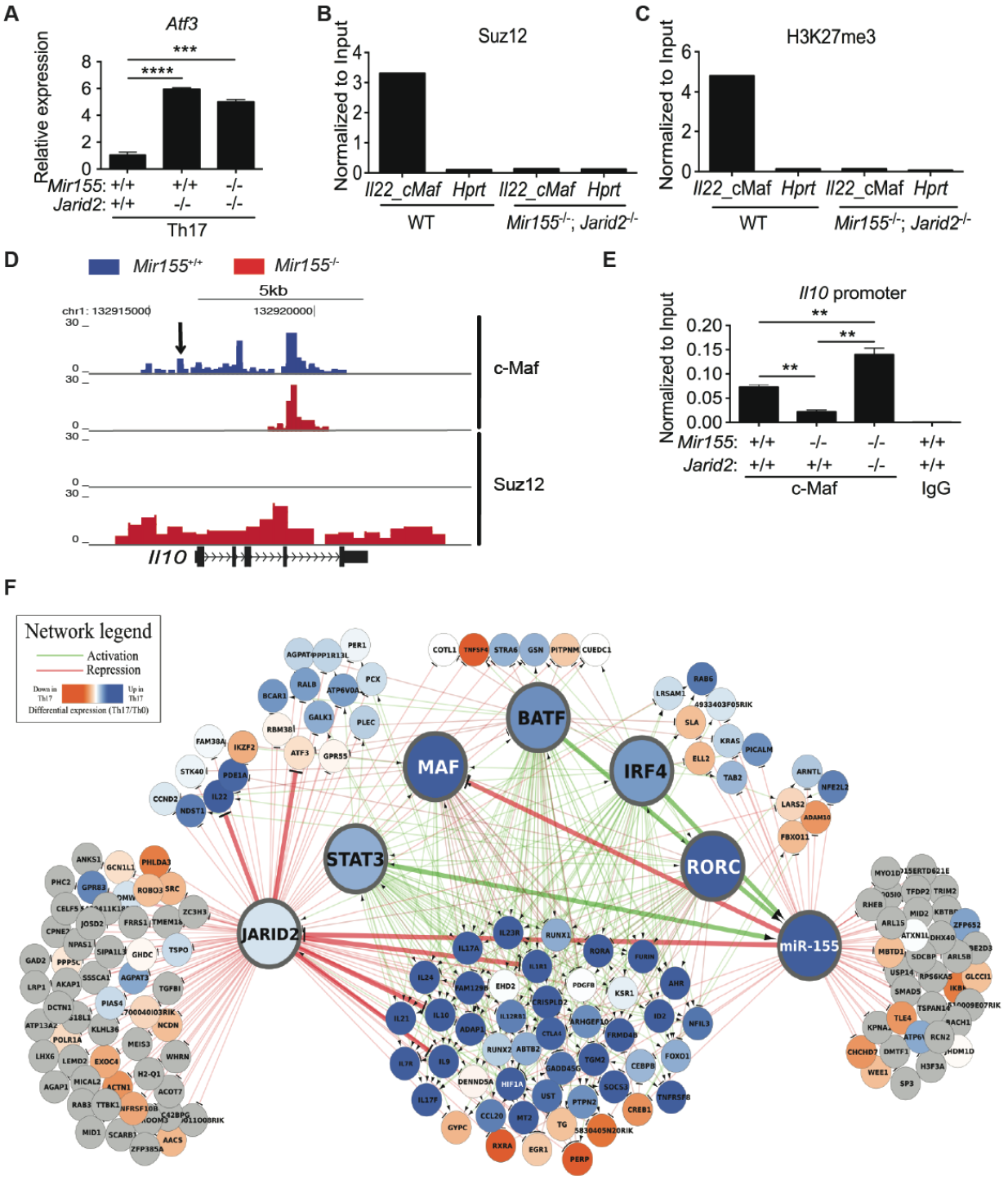

Figure S7, related to Figure 7. Profiling PRC2 and c-Maf binding at *Il22* and *Il10* locus in *Mir155*$^{-/-}$, double-deficient *Mir155*$^{-/-}$; *Jarid2*$^{-/-}$ and WT Th17 cell cultures, and updated Th17 network. (A) RT-qPCR of *Atf3* in *Jarid2*$^{-/-}$, *Mir155*$^{-/-}$; *Jarid2*$^{-/-}$, and littermate controls. Relative

expression was found by normalizing to *Gapdh* mRNA. (C-B) ChIP-qPCR for Suz12 (B) and H3K27me3 (C) enrichment on the *Il22* promoter where c-Maf binds (denoted as *Il22_cMaf*) or *Hprt* promoter in WT or *Mir155*$^{-/-}$; *Jarid2*$^{-/-}$ Th17 cell cultures normalized to input controls. (D) Genome browser screenshots Suz12 and c-Maf enrichment in the *Mir155*$^{-/-}$ and *Mir155*$^{+/+}$ Th17 cell cultures. Black arrow marks a previously reported c-Maf binding site that activates *Il10* transcription (Xu et al., 2009). (E) ChIP-qPCR of c-Maf on the *Il10* promoter in *Mir155*$^{-/-}$**,** *Mir155*$^{-/-}$**;** *Jarid2*$^{-/-}$, and WT Th17 cell cultures normalized to input controls. ChIP-qPCR in WT Th17 cell cultures using an IgG control is included. Statistical significance determined using unpaired Student's *t* test (** $p<0.01$). (E) An updated Th17 regulatory network that integrates miR-155 and Jarid2.

Extended Experimental Procedures

Cell isolation and flow cytometry

For the isolation of siLP lymphocytes, small intestine was collected in ice-cold HBSS buffered in 25 mM HEPES with 5% FBS. Then, intestine was opened longitudinally and cut into small pieces. Tissue fragments were washed once with HBSS containing 2 mM EDTA and 25mM HEPES followed by 37°C with shaking in HBSS containing 10% FBS, 5 mM EDTA, 15 mM HEPES and 0.015% DTT. Next, the tissue was washed 5 times with HBSS containing 25 mM HEPES and 5% FBS and digested with Liberase TL (0.17 mg/ml) and DNAse (30 μg/ml) in pre-warmed Iscove's Complete Media containing 5% FBS followed by 30-60 minutes at 37°C with shaking. Digested intestines were washed with HBSS containing 25 mM HEPES and 5% FBS followed by passing tissue through a 70-μm and 40-μm strainer (BD Biosciences).

We used the AS15 I-A^b tetramer (Grover et al., 2012) labeled with APC and loaded with the *T. gondii* peptide (AVEIHRPVPGTAPPS) prepared by NIH Tetramer Core Facility (Emory University). After cell stimulation, cells were first stained with tetramer for 1 hour at 37°C and then processed with rest of samples.

Mouse T helper cell differentiation

Single-cell suspensions were prepared from spleens and lymph nodes by mechanical disruption and filtering through 40-μm cell strainers (BD Biosciences). Naïve T cells were either sorted using BD FACS Aria cell sorter using the markers $CD4^+CD44^-CD62L^{high}CD25^-$ or were positively selected for CD4 using Miltenyi Biotec AutoMACS. Cells were co-cultured with irradiated (3000 Rads) T cell-depleted splenocytes in the presence of 1 μg/ml of anti-CD3 and 1μg/ml of anti-CD28 for 4 days with various combinations of antibodies and cytokines: for Th1 conditions, 10 ng/ml of IL-12 and 10 μg/ml of anti-IL-4; for Th2 conditions, 10ng/ml of IL-4, 10 ng/ml of IL-2, 10 μg/ml anti-IL-12 and anti-IFN-γ; for Th17 conditions 10 ng/ml of IL-6, 10 ng/ml of IL-21, and 0.5 ng/ml of TGFβ with 10 μg/ml of anti-IL-4, anti-IL-12 and anti-IFN-γ; for iTregs, 50 U/ml of IL-2, 10 μg/ml of TGFβ with 10 μg/ml of antil-IL-4, anti-IFN-γ, and anti-IL-12 for Th0 conditions 10 μg/ml of anti-IL-4, anti-IL-12 and anti-IFN-γ with no cytokines. For Th17 culturing conditions, 10% FBS in RPMI (GIBCO) was used and when indicated 10 ng/ml of IL-1β was also added. For mouse cultures, all recombinant cytokines were purchased from R&D and blocking antibodies and crosslinking antibodies were purified from hybridomas (Harlan).

Human T helper cell differentiation

Human peripheral blood mononuclear cells (PBMCs) were prepared from 20- to 60-year-old healthy donors by the Department of Transfusion Medicine at NIH. The acquisition of blood products was approved according to the Institutional Review Board, and in accordance with the Declaration of Helsinki. Naïve $CD4^+$ T cells were first sorted using the $CD4^+CD25^-CD45RA^+$ markers. For T helper subset skewing, 24-well plates were coated overnight at 4°C or 4 hours at 37°C with 2 μg/ml in PBS containing anti-CD3 and anti-CD28. The cells were cultured with 10% FBS IMDM (GIBCO) for 5-6 days along with respective cytokine cocktail. If necessary, cells were split after 3 days with similar cocktail of antibodies. For Th1 condition: 1 ng/ml of IL-12, 50 U/ml of IL-2 with 1 μg/ml of anti-IL-4; for Th2 condition, 20 ng/ml of IL-4, 50 U/ml of IL-2 with 1 μg/ml of anti-IL-12 and anti-IFN-γ; For iTreg condition, 50 U/ml of IL-2, 10ug/ml of TGFβ with 1 μg/ml of anti-IL-4 and anti-IFN-γ; For Th17 condition, 50 U/ml of IL-2, 10ng/ml of each IL-1β, IL-6, IL-23, 10 ng/ml of TGFβ, with 1μg/ml of anti-IL-4 and anti-IFN-γ. For human cultures, all recombinant cytokines were purchased from Peprotech and blocking antibodies for IL-12, IL-4, IFN-γ were affinity-purified polyclonal goat IgG from R&D Systems.

Retroviral Cloning and Transductions

Mouse *Atf3* was PCR amplified from a cDNA clone obtained from Origene (MC201919) and subcloned into the MSCV-IRES-GFP vector provided by Ken Murphy (Washington University). Plasmid insert was verified by sequencing and retroviral supernatants were generated. After the first 24 hours, Th17 cultures were transduced by spin-infection at 700xg for 90 minutes at 32°C in the presence of retroviral supernatant and 5 μg/mL polybrene (Sigma-Aldrich). Cells were returned to incubator for another 6 hours and then viral media was replaced with fresh media.

Th17 polarization was then continued for 3 days followed by re-stimulation with PMA and Ionomycin in the presence of Golgi block for 4 hours. Transduced Th17 cell cultures were then fixed with 1% Paraformaldehyde (Electron Microscopy Sciences) followed by intracellular cytokine staining in 1xPBS with 0.1% TritonX100 (Sigma-Aldrich).

RNA-seq analysis.

Reads from single or paired-end RNA-seq were mapped to the mouse genome (NCBI 37, mm9) using the splice-aware aligner TopHat (version-1.3.1)c(Trapnell et al., 2009) with option --mate-inner-dist 160 --coverage-search --microexon-search --max-multihits 20. In short, using a two-step mapping processes TopHat first calls Bowtie (version-0.12.7) (Langmead et al., 2009) to align reads that are directly mapped to the reference genome (with no gaps). Bowtie then determines the possible location of gaps in the alignment based on canonical and non-canonical splice sites flanking the aligned reads. Finally, Bowtie uses gapped alignments to align the reads that were not aligned in the first step. Aligned reads were then visualized on a local mirror of the UCSC Genome Browser (Kent et al., 2002).

Differentially expressed gene and miRNA signature analyses.

Gene expression quantification was performed by counting aligned reads on each gene for each condition using in-house codes. DEGseq (Wang et al., 2010) was then applied to identify differentially expressed genes between two conditions with addition options *p value* threshold 1e-5 and fold change threshold 1.4. To identify putative target genes, a ranked gene list from up-regulated to down-regulated based on the $\log_2$ of the ratio of the expression level of each gene in the two conditions was supplied to Sylamer (van Dongen et al., 2008) to statistically calculate

the enrichment of seed sequences of all known miRNAs (version 15 from miRbase.org). A list of 220 putative target genes were identified by choosing up-regulated genes containing miR-155 seed sequences (AGCATTA and GCATTAA) that pass the E-value threshold (Bonferroni-corrected) of *p value* < 0.01. Comparisons this putative target gene list against 134 and 256 putative miR-155 target mRNAs phylogenetically predicted by PicTar (http://pictar.mdc-berlin.de/)(Krek et al., 2005) and TargetScan (http://www.targetscan.org/)(Lewis et al., 2003) gave 15 putative miR-155 target mRNAs in common among the three methods (see Figure 4B). The False Discovery Rate (FDR) of the overlapped genes was then estimated by shuffling the RefSeq gene list 1000 times, randomly picking up 134 and 256 genes and getting the average number of genes that overlap with the Sylamer miR-155 target gene list, which are 1.4 and 2.5 respectively. The FDR for the overlapped genes (1.4 out of 25 and 2.5 out of 42 genes) then is about 6% for both comparisons.

ChIP-seq and ChIP-exo analysis.

Reads from ChIP-seq were mapped to the mouse genome (NCBI 37, mm9) using the short read, memory efficient aligner Bowtie (version-0.12.7)(Langmead et al., 2009) with option -p 8 --chunkmbs 256 -a --best --strata -m 20. Unique reads are considered by instructing Bowtie to refrain from reporting any alignments for reads that have more than 20 reportable alignments. Reads from ChIP-exo were mapped by Peconic (State College, PA) to the mouse genome (NCBI 37, mm9) using BWA (version 0.5.9) with default options allowing one gap open and a maximum number of three alignments for any read that aligned across the genome. Sub-module of SICER (version-1.1)(Zang et al., 2009) was used on BED files containing the unique reads to determine window size (Abraham et al., 2013) for Jarid2, Suz12, and H3K27me3. The window

sizes for each ChIP-seq were as follows: Jarid2 was 2102 bp; Suz12 was 397 bp; while H3K27me3 had a window size of 2852 bp. SICER-df.sh was used for Suz12, Jarid2 and H3K27me3 analysis with a gap size of 0 for Jarid2, Suz12, and H3K27me3. All SICER-df.sh analysis had an FDR cutoff of 0.01. For ChIP-exo analysis, SICER-rb.sh was used to find enriched Jarid2 and Suz12 islands with an E value cut-off of 0.1, a window size of 50 and a gap size of 100. For c-Maf analysis, MACS (Version 1.4.2) was used for c-Maf binding enrichment using the following parameters "–f BED –g mm –p 1E-5 –w –S" using the duplicates processed BED files of c-Maf-miR-155-WT against c-Maf-miR155-WT-Input and c-Maf-miR-155-KO against c-Maf-miR155-KO-Input.

For comparison of KO vs WT, MACS2 (Version-2.0.9) was used with the following parameters "–f BED –g mm –p 1E-5 –B" against the duplicates processed BED files. The output from MACS2.0 was used with a sub-module of MACS2 "bdgdiff", tool that identifies differential binding regions, with a minimum peak length of 200, differential peak consideration cutoff of 5 and a gap size between any two peaks to be 30.

For visualization of RNA-seq, ChIP-seq, and ChIP-exo tracks, wiggle files were generated from BAM files using custom Python scripts and then provided to D-Peaks (Brohee and Bontempi, 2012) to plot the coverage tracks (tags per million) at specified locations on the genome.

Th17 Network.

The KCRI Th17 cell specification regulatory network (Ciofani et al., 2012) was downloaded from http://th17.bio.nyu.edu/pages/cytoscape.html. Targets of miR-155 and Jarid2-PRC2 were integrated in to the KCRI network to generate an updated Th17 regulatory network. Associations

between transcription factors and miR-155 were added based on available ChIP-seq evidence. Network data integration, visualization and analysis were performed using the Cytoscape platform (Smoot et al., 2011). Genes (nodes) are colored based on the level of differential expression (orange to blue correspond to low to high Th17 expression relative to Th0; grey denotes missing expression data). Edges (associations) are colored as either activation (green) or repression (red). Nodes with many associations are denoted by large circles. Nodes with 4 or more connections are grouped in the middle, whereas those with fewer connections are in the periphery.

List of antibodies used in this study

Antigen	Antibody	Applications and dilutions	Source
c-Maf	Rabbit (M-153)	WB (1:1000); 2μg in ChIP	Santa Cruz
Jarid2	Rabbit (ab48137)	WB (1:1000); 2μg in ChIP	Abcam
Suz12	Rabbit (C39F6)	2μg in ChIP	Cell Signaling
H3K4me3	Rabbit (CS200580)	2μg in ChIP	Millipore
H3K27me3	Rabbit (07-449)	2μg in ChIP	Millipore
RNA Pol II	Mouse (4H9)	2μg in ChIP	Abcam
CD4 (human)	Mouse (S3.5)	1:200 Flow	BD
CD4	Rat (RM4-5)	1:400 Flow	eBioscience
CD3ε (human)	Mouse (UCHT1)	2μg/ml for cross-linking	BD
CD3ε	Rat (2C11)	1μg/ml for cross-linking	Harlan
CD28 (human)	Mouse (CD28.2)	2μg/ml for cross-linking	BD
CD28	Rat (37.51)	1μg/ml for cross-linking	Harlan
CD25 (human)	Mouse (CD25-3G10)	1:200 Flow	BD
CD45RA (human)	Mouse (MEM-56)	1:200 Flow	BD
CD44	Rat (IM7)	1:400 Flow	eBioscience
CD8a	Rat (53-6.7)	1:400 Flow	eBioscience
Foxp3	Rat (FJK-16s)	1:200 Flow	eBioscience
IL-17A	Rat (eBio17B7)	1:400 Flow	eBioscience
IFN-γ	Rat (XMG1.2)	1:400 Flow; 10μg/ml for neutralization	eBioscience; Harlan
IL-12p40	Rat (C17.8)	10μg/ml for neutralization	Harlan
IL-4	Rat (11B11)	1:400 Flow; 10μg/ml for neutralization	eBioscience; Harlan

RORγt	Rat (AFKJS-9)	1:200 Flow	eBioscience
BATF	Mouse (MBM7C7)	1:200 Flow	eBioscience
IRF4	Rat (3E4)	1:200 Flow	eBioscience
TCRβ	Hamster (H57-597)	1:200 Flow	eBioscience
CD45.2	Mouse (104)	1:200 Flow	eBioscience
CD45.1	Mouse (A20)	1:200 Flow	eBioscience

List of TaqMan Probes for RT-PCR
(all from Applied Biosystems except for *Atf3* and *Jarid2* Exon 3 which are from IDT)

Gene Name	Probe
Il22	Mm00444241_m1
Il17a	Mm00439619_m1
Il17f	Mm00521423_m1
Il9	Mm00434405_m1
Il10	Mm01288386_m1
Rorc (RORγt)	Mm00441139_m1
Ahr	Mm00478930_m1
Batf	Mm01307960_m1
Jarid2	Mm00445560_m1
Cyp1a1	Mm00487217_m1
Il1r1	Mm00434237_m1
Irf4	Mm00516431_m1
hsa-miR-155	002623
mmu-miR-155	002571
U6	001973
Gapdh	Mm99999915_g1
Atf3	Primer 1: TCTGGCCGCTCTCTGGA Primer 2: GCGGTCGCACTGACTTCT FAM/Tam Probe: TTCAACATCCAGGCCAGGTCTCTG
Jarid2 exon 3	Primer 1: ATGACAGCGATGGGATCC Primer 2: GCTGCCTTTTCTGTGCATTC FAM/Tam Probe: TCGTACAACTCTCTCTTCTGACCACGG/

Mouse primers for ChIP-qPCR, intronic RT-qPCR and Genotyping

Gene region	Forward primer (5'→3')	Reverse Primer (5'→3')
Il22 TSS	GAACATGCTCCCCTGATGTT	CAGAGATCGCACAAGTGTCAA
Il10 promoter	TAAGAGCAGGCAGCATAGCA	AAAAGGGGGACCAAGAACAG
Il9 promoter	AGAGCAAAACAGAGGCAAGG	AAGTGGGCACTGGGTATCAG

Il22 promoter	TGCAATCAATCCCAGTATTTTG	CTTGTGCAAGCATAAGTCTCAA
Il22 proximal	GTGTGCTTGGCTTCTTCAGG	GTGTGCTTGGCTTCTTCAGG
Il22 distal	TACCAGGAGCCACTTCCTTG	TACCAGGAGCCACTTCCTTG
Il22 c-Maf site	GTTGGTGGGAAAATGAGTCC	CATGGCTTTGCCGTAGTAGA
Il10 c-Maf site	CTCTCCTCTGACCAACTGCC	TGGGTTGAACGTCCGATATT
Il17a promoter	GCACTTTACCTCCCCAGCTT	TTCCCTGGCTAGAGAGCATC
Hprt promoter	CTGCCTCTGCCTCCTAAATG	AGGCCCAGTTCTTTCACAAA
Il9 intron 3	AATGTCACTGGGAAACTGACCT	CCTAGGACTGCTTTCAGGAAGA
Il22 intron 4	AGGGGGACTTGCTTTGCCATTT	AACACCCCTTCTTTCCTCCTCCAT
CD4cre Genotyping	CCCAACCAACAAGAGCTC	CCCAGAAATGCCAGATTACG
Jarid2 floxed	TAGTCAGGGCAAGGTGGAAG	TCCCAACCTTCCTAATGCT

Supplemental References

Abraham, B.J., Cui, K., Tang, Q., and Zhao, K. (2013). Dynamic regulation of epigenomic landscapes during hematopoiesis. BMC Genomics *14*, 193.

Brohee, S., and Bontempi, G. (2012). D-peaks: A visual tool to display ChIP-seq peaks along the genome. Transcription *3*.

Grover, H.S., Blanchard, N., Gonzalez, F., Chan, S., Robey, E.A., and Shastri, N. (2012). The Toxoplasma gondii peptide AS15 elicits CD4 T cells that can control parasite burden. Infect Immun *80*, 3279-3288.

Kent, W.J., Sugnet, C.W., Furey, T.S., Roskin, K.M., Pringle, T.H., Zahler, A.M., and Haussler, D. (2002). The human genome browser at UCSC. Genome Res *12*, 996-1006.

Langmead, B., Trapnell, C., Pop, M., and Salzberg, S.L. (2009). Ultrafast and memory-efficient alignment of short DNA sequences to the human genome. Genome Biol *10*, R25.

Mysliwiec, M.R., Chen, J., Powers, P.A., Bartley, C.R., Schneider, M.D., and Lee, Y. (2006). Generation of a conditional null allele of jumonji. Genesis *44*, 407-411.

Smoot, M.E., Ono, K., Ruscheinski, J., Wang, P.L., and Ideker, T. (2011). Cytoscape 2.8: new features for data integration and network visualization. Bioinformatics *27*, 431-432.

Trapnell, C., Pachter, L., and Salzberg, S.L. (2009). TopHat: discovering splice junctions with RNA-Seq. Bioinformatics *25*, 1105-1111.

Wang, L., Feng, Z., Wang, X., and Zhang, X. (2010). DEGseq: an R package for identifying differentially expressed genes from RNA-seq data. Bioinformatics *26*, 136-138.

Zang, C., Schones, D.E., Zeng, C., Cui, K., Zhao, K., and Peng, W. (2009). A clustering approach for identification of enriched domains from histone modification ChIP-Seq data. Bioinformatics *25*, 1952-1958.